

Numerical Simulation of Low-Speed Gas Flows in a Microfluidic System

Chan H. Chung*

Daegu University, Gyungsan, Gyungbuk, 712-714, Republic of Korea

A kinetic theory analysis is made of low-speed gas flows in microfluidic systems consisting of microchannels in series. The Boltzmann equation, simplified by a collision model, is solved by means of a finite difference approximation with the discrete ordinate method. For the evaluation of the present method, the results for simple channels are compared with those from several different methods and available experimental data. Calculations are made for various microfluidic systems such as a sudden expansion, a sudden contraction, and a 90-deg bend. The results compared well with those from the discrete simulation Monte Carlo method. The present method does not suffer from the statistical noise that is common in particle-based methods, and it requires a smaller amount of computational effort. It is also shown that the analytical solution of the Navier–Stokes equations with slip boundary conditions, which is suitable for fully developed flows, can give relatively good results in predicting geometrically complex flows such as a sudden expansion and a sudden contraction.

Nomenclature

A_c	= collision frequency
d	= characteristic length of the flowfield
F	= Maxwell–Boltzmann distribution
f	= distribution function
g, h	= reduced distribution functions
Kn	= Knudsen number
λ	= mean free path

Subscripts

d	= exit condition
0	= inlet condition

I. Introduction

MICROCHANNELS are important components of microelectromechanical systems (MEMS), which have been the subject of increasingly active research during the last three decades. The length scale of microchannels in MEMS devices is typically on the order of micrometers. The Knudsen number of the flowfield, or the ratio of the mean free path to the characteristic channel dimension, is usually not negligibly small even at atmospheric operating conditions. Hence, conventional computational fluid dynamics methods that are based on continuum assumptions may not be appropriate, and a method based on kinetic gas theory is required to describe the flows accurately.

Of the various methods available for the analysis of microchannel flows, the direct simulation Monte Carlo (DSMC) method¹ has been used by many researchers.^{2–5} The DSMC method has been known to be a robust and accurate method because it is based on kinetic gas theory and does not rely on the continuum assumption that is not valid for high Knudsen number gas flows. Even though the DSMC method has been successfully applied for the analysis of various kind of rarefied gas flows, the simulation of low-speed microchannel flows using the DSMC method suffers from several difficulties, including large statistical scatter that has not been encountered in the high-speed gas flow simulations. To get a meaningful result by

reducing the large statistical noise, the DSMC method requires a vast amount of computational effort due to the number of time steps needed to reach the steady-state flow condition and the large sample size.⁴ These computational demands can render the standard DSMC method impractical given current computing power limitations. Because of the difficulties, most of the reported DSMC simulations have dealt with simple microchannels with a very small length-to-height (L/H) ratio and a relatively large pressure ratio.

An alternate approach is the information preservation (IP) method developed by Fan and Shen.⁶ The IP method preserves macroscopic information while the flowfield is simulated by the DSMC method. The method has been applied to various types of low-speed flow problems.^{7–10} Even though the IP method has been reported to reduce the sampling size by orders of magnitude, the method still requires a large amount of computing effort.

In the present study, a finite difference method coupled with the discrete-ordinate method^{11,12} is employed to analyze low-speed gas flows in microfluidic systems consisting of microchannels in series. In the method, the Boltzmann equation, simplified by a collision model [Bhatnagar–Gross–Krook (BGK) equation]¹³ is solved by means of a finite difference approximation. The physical space is transformed by a general grid-generation technique. The velocity space is transformed to a polar coordinate, and the concept of the discrete ordinate method is employed to discretize the velocity space. The modified Gauss–Hermite quadrature (see Refs. 14 and 15) and Simpson's rule are used for the integration of the discretized velocity space.

To assess the present method, calculations are made for simple microchannel flows, and results are compared with those from the DSMC method, an analytical solution of the Navier–Stokes equations with slip boundary conditions (see Ref. 16), and available experimental data. Then the method is applied to various microfluidic systems such as a sudden expansion, a sudden contraction, and a 90-deg bend.

II. Finite Difference Method

A. Governing Equation

We consider the steady-state Boltzmann equation with the BGK model¹³ in a two-dimensional Cartesian coordinate system

$$V_x \frac{\partial f}{\partial x} + V_y \frac{\partial f}{\partial y} = A_c (F - f) \quad (1)$$

where $f(x, y, V_x, V_y, V_z)$ is the distribution function; x and y are Cartesian coordinates of the physical space; V_x , V_y , and V_z are the velocity components of the molecules; and A_c is the collision

Received 20 June 2004; presented as Paper 2004-2675 at the AIAA 37th Thermophysics Conference, Portland, OR, 28 June–1 July 2004; revision received 12 September 2004; accepted for publication 12 September 2004. Copyright © 2004 by the American Institute of Aeronautics and Astronautics, Inc. All rights reserved. Copies of this paper may be made for personal or internal use, on condition that the copier pay the \$10.00 per-copy fee to the Copyright Clearance Center, Inc., 222 Rosewood Drive, Danvers, MA 01923; include the code 0887-8722/05 \$10.00 in correspondence with the CCC.

*Professor, Department of Chemical Engineering. Member AIAA.

frequency. The equilibrium Maxwell–Boltzmann distribution F is given by

$$F = n(2\pi RT)^{-\frac{3}{2}} \exp[-(V - U)^2/2RT] \quad (2)$$

The moments n , U , and T can be obtained by integrating the distribution function over the velocity space:

$$n = \int f \, dV \quad (3a)$$

$$nU = \int Vf \, dV \quad (3b)$$

$$3nRT = \int (V - U)^2 f \, dV \quad (3c)$$

where R denotes the gas constant, n the particle density, and U the macroscopic flow velocity.

The following reduced distribution functions are introduced to reduce the number of independent variables:

$$g(x, y, V_x, V_y) = \int_{-\infty}^{+\infty} f(x, y, V_x, V_y, V_z) \, dV_z \quad (4a)$$

$$h(x, y, V_x, V_y) = \int_{-\infty}^{+\infty} V_z^2 f(x, y, V_x, V_y, V_z) \, dV_z \quad (4b)$$

These kinds of reduced distribution functions were first applied by Chu¹⁷ and have been employed by many researchers. The corresponding equations for the reduced distribution functions are obtained by integrating out the V_z dependence with the weighting functions 1 and V_z^2 , respectively:

$$V_x \frac{\partial g}{\partial x} + V_y \frac{\partial g}{\partial y} = A_c(G - g) \quad (5a)$$

$$V_x \frac{\partial h}{\partial x} + V_y \frac{\partial h}{\partial y} = A_c(H - h) \quad (5b)$$

$$G(x, y, V_x, V_y) = \int_{-\infty}^{+\infty} F \, dV_z \quad (5c)$$

$$H(x, y, V_x, V_y) = \int_{-\infty}^{+\infty} V_z^2 F \, dV_z \quad (5d)$$

By the use of the characteristic length of a flowfield d and the most probable speed V_0 , defined as

$$V_0 = \sqrt{2RT_0} \quad (6)$$

the following dimensionless variables are introduced:

$$\begin{aligned} \hat{x} &= x/d, & \hat{y} &= y/d, & \hat{n} &= n/n_0, & \hat{V}_i &= V_i/V_0 \\ \hat{U}_i &= U_i/V_0, & \hat{T}_i &= T_i/T_0, & \hat{A}_c &= \hat{A}_c d/V_0 \\ \hat{g} &= gV_0^2/n_0, & \hat{h} &= h/n_0, & \hat{G} &= GV_0^2/n_0 \\ \hat{H} &= H/n_0, & \hat{\tau} &= \tau/(1/2mn_0U_\infty^2) \end{aligned} \quad (7)$$

where the subscript 0 refers to a reference condition.

By the introduction of a polar coordinate system, which is defined as

$$\hat{V}_x = V \sin \phi, \quad \hat{V}_y = V \cos \phi, \quad \phi = \tan^{-1}(\hat{V}_x/\hat{V}_y) \quad (8)$$

and by the application of general transform rules, the governing equations in the new coordinate system (ξ, η) are written as¹⁸

$$B \frac{\partial \hat{g}}{\partial \eta} + C \frac{\partial \hat{g}}{\partial \xi} = \hat{A}_c(\hat{G} - \hat{g}) \quad (9a)$$

$$B \frac{\partial \hat{h}}{\partial \eta} + C \frac{\partial \hat{h}}{\partial \xi} = \hat{A}_c(\hat{H} - \hat{h}) \quad (9b)$$

$$B = \frac{(\hat{x}_\xi \cos \phi - \hat{y}_\xi \sin \phi)V}{J_t} \quad (9c)$$

$$C = \frac{(\hat{y}_\eta \sin \phi - \hat{x}_\eta \cos \phi)V}{J_t} \quad (9d)$$

Here, J_t denotes the Jacobian of the transformation.

B. Discrete Ordinate Method

To remove the velocity-space dependency from the reduced distribution functions, the discrete ordinate method^{14,15} is employed. This method, which consists of replacing the integration over velocity space of the distribution functions by appropriate integration formulas, requires the values of the distribution functions only at certain discrete speeds and velocity angles. By employment of discrete distribution functions $\hat{g}_{\delta\sigma}(\xi, \eta, V_\delta, \phi_\sigma)$ and $\hat{h}_{\delta\sigma}(\xi, \eta, V_\delta, \phi_\sigma)$ for the discrete speed V_δ and velocity angle ϕ_σ , the macroscopic moments given by integrals over the molecular velocity space can be substituted by the following quadratures:

$$\hat{n} = \sum_\delta \sum_\sigma P_\delta P_\sigma \hat{g}_{\delta\sigma} \quad (10a)$$

$$\hat{n}\hat{U}_x = \sum_\delta \sum_\sigma P_\delta P_\sigma V_\delta \sin \phi_\sigma \hat{g}_{\delta\sigma} \quad (10b)$$

$$\hat{n}\hat{U}_y = \sum_\delta \sum_\sigma P_\delta P_\sigma V_\delta \cos \phi_\sigma \hat{g}_{\delta\sigma} \quad (10c)$$

$$\frac{3\hat{n}\hat{T}}{2} = \sum_\delta \sum_\sigma P_\delta P_\sigma (h_{\delta\sigma} + V_\delta^2 \hat{g}_{\delta\sigma}) - \hat{n}(\hat{U}_x^2 + \hat{U}_y^2) \quad (10d)$$

where P_δ and P_σ are weighting factors of the quadratures for the discrete speed V_δ and velocity angle ϕ_σ , respectively. Thus, instead of solving the equations for a function of space and molecular velocity, the equations are transformed to partial differential equations that are continuous in space but that are point functions in molecular speed V_δ and velocity angle ϕ_σ as follows:

$$B_{\delta\sigma} \frac{\partial \hat{g}_{\delta\sigma}}{\partial \eta} + C_{\delta\sigma} \frac{\partial \hat{g}_{\delta\sigma}}{\partial \xi} = \hat{A}_c(\hat{G}_{\delta\sigma} - \hat{g}_{\delta\sigma}) \quad (11a)$$

$$B_{\delta\sigma} \frac{\partial \hat{h}_{\delta\sigma}}{\partial \eta} + C_{\delta\sigma} \frac{\partial \hat{h}_{\delta\sigma}}{\partial \xi} = \hat{A}_c(\hat{H}_{\delta\sigma} - \hat{h}_{\delta\sigma}) \quad (11b)$$

$$B_{\delta\sigma} = \frac{(\hat{x}_\xi \cos \phi_\sigma - \hat{y}_\xi \sin \phi_\sigma)V_\delta}{J_t} \quad (11c)$$

$$C_{\delta\sigma} = \frac{(\hat{y}_\eta \sin \phi_\sigma - \hat{x}_\eta \cos \phi_\sigma)V_\delta}{J_t} \quad (11d)$$

C. Collision Frequency

The simplest model for the collision integral is the BGK model,¹³ which has been widely used and generally gives reasonable results with much less computational effort. In the BGK model, the collision frequency is given by

$$A_c = \psi(P/\mu) \quad (12)$$

where the quantity ω is the viscosity index and ψ is a numerical parameter. The coefficient of viscosity μ is assumed to have a temperature dependency¹⁹

$$\mu/\mu_0 = (T/T_0)^\omega \quad (13)$$

The equilibrium mean free path for the variable hard sphere (VHS) model²⁰ is employed

$$\lambda_0 = \frac{16}{5} \frac{F_k \mu_0}{m n_0 \sqrt{2\pi R T_0}} \quad (14)$$

where the quantity F_k is given by

$$F_k = \frac{(5 - 2\omega)(7 - 2\omega)}{24} \quad (15)$$

Combining Eqs. (12–15), we obtain

$$\hat{A}_c = \frac{8\psi F_k \hat{n} \hat{T}^{1-\omega}}{5\sqrt{\pi} K n_0} \quad (16)$$

where $K n_0$ is the Knudsen number at the reference condition based on the characteristic length of the flowfield d .

D. Numerical Procedure

Equations (11a) and (11b) are solved by means of finite difference approximations in physical space using simple explicit and implicit schemes, depending on the characteristics of physical and velocity space. Details of the method can be found elsewhere.¹⁸ The resulting system of nonlinear algebraic equations is solved by means of successive approximations. In the iterative procedure, only the values of \hat{A}_c , $\hat{G}_{\delta\sigma}$, and $\hat{H}_{\delta\sigma}$ have to be determined from moments of the preceding iteration, and the values of distribution functions do not need to be stored. Convergence is assumed to have occurred when the relative differences in the x velocities of two successive iteration steps are less than 10^{-5} for all spatial grid points. As a proper quadrature formula for the discrete speed V_δ , the modified Gauss–Hermite half-range quadrature for integrals of the form from Refs. 14 and 15 is used:

$$\int_0^\infty V^j \exp(-V^2) Q(V) dV = \sum_{\delta=1}^N P_\delta Q(V_\delta) \quad (17)$$

E. Boundary Conditions

The following boundary conditions are used for the calculation. At inlet and exit boundaries, the distribution functions are given by an equilibrium distribution with prescribed conditions:

$$f_b = n_b (2\pi R T_b)^{-\frac{3}{2}} \exp\left[-(V - U_b)^2 / 2 R T_b\right] \quad (18)$$

where the subscript b refers to conditions at the boundaries.

To specify the interaction of the molecules with the surface, diffuse reflection is assumed, that is, molecules that strike the surface are subsequently emitted with a Maxwell distribution characterized by the surface temperature T_w , for $(V \cdot \tilde{n}) < 0$,

$$f_w = \tilde{n}_w (2\pi R T_w)^{-\frac{3}{2}} \exp\left[-(V - U_w)^2 / 2 R T_w\right] \quad (19)$$

where the subscript w refers to conditions at the surface, and \tilde{n} is the inward normal vector to the surface. The wall number flux \tilde{n}_w is not known a priori and may be determined by applying the condition of no net flux normal to the surface:

$$\int_{(V \cdot \tilde{n}) > 0} (V \cdot \tilde{n}) f dV = - \int_{(V \cdot \tilde{n}) < 0} (V \cdot \tilde{n}) f_w dV \quad (20)$$

III. DSMC Method

The DSMC method is a popular simulation technique for low-density flows, and the DSMC code used in the present study is based on the same principles as described by Bird,¹ together with the VHS model²⁰ as a molecular model and the no time counter method²¹ as a collision sampling technique. The code has been applied to various low-density flows of gas mixtures in arbitrary shaped flow domains.^{22,23} Details of the code may be found in Ref. 22.

IV. Results and Discussion

A low-speed, two-dimensional gas flow through a simple microchannel with a dimension of $0.5(H) \times 15(L) \mu\text{m}$ is considered first (case 1). The gas is air with the viscosity index of $\omega = 0.77$. The pressures at the inlet and the exit are 2.5×10^5 and 1.0×10^5 Pa, respectively. The temperature at the inlet is 300 K. The diffuse boundary condition at the wall temperature of 300 K is used. The average Knudsen number calculated using the flow variables at the mean pressure $P = (P_0 + P_d)/2$ is $Kn = 0.06$. The exponent j and the order of the quadrature N in Eq. (17) are chosen to be 1 and 16, respectively. Simpson's three-eighth rule with $\Delta\phi = \pi/30$ is used for the discrete velocity angle. The BGK model parameter ψ was chosen to be 1.3 for the problems considered in the present study. In the case of the hard sphere molecules, the BGK model parameter ψ usually assumed to be between two-thirds and one (Ref. 24) from the well-known behavior of the BGK model, which requires further investigation. At the inlet and outflow boundaries, the pressure boundary condition adopted by Nance et al.⁵ is used to correct the variables at the boundaries both for the present and the DSMC methods. For the calculations, only the upper-half portion of the flow domain is considered, with a symmetric boundary condition along the centerline. For the DSMC calculation, a rectangular grid system of 330×25 cells is employed with about 240,000 particles and 35,000 sampling time steps (average sampling size of 1.0×10^6 per cell) after 30,000 time steps of development. For the present method, a rectangular grid system of 331×26 grids is employed. CPU times required for the DSMC and the present methods were about 30.2 and 9.1 h, respectively. All of the calculations in the present work are performed on a desktop computer with a Pentium IV 3.0-GHz processor.

Figure 1 shows x -velocity profiles at $x/L = 0.2, 0.4, 0.6$, and 0.8 from the present and the DSMC methods, together with those from the analytical solution of the Navier–Stokes equations with slip boundary conditions.¹⁶ Details of the analytical solution of the Navier–Stokes equations (A-NS in Fig. 1) may be found in Ref. 16. Note that the results from the present method compare very well with those from the DSMC method. The results from the analytical solution of the Navier–Stokes equations compare relatively well, except for some differences near the surface.

The next problem considered is a low-speed, two-dimensional flow through a simple microchannel with a dimension of $1.2(H) \times 3000(L) \mu\text{m}$. The gas is air with the viscosity index of $\omega = 0.7$. The pressures at the inlet and the exit are 2.3918×10^5 and 1.0133×10^5 Pa, respectively. It is the shortest microchannel investigated experimentally. It is also the one with the largest L/H ratio among those investigated using particle-based methods.⁷ The coefficient of viscosity of nitrogen at the reference temperature of

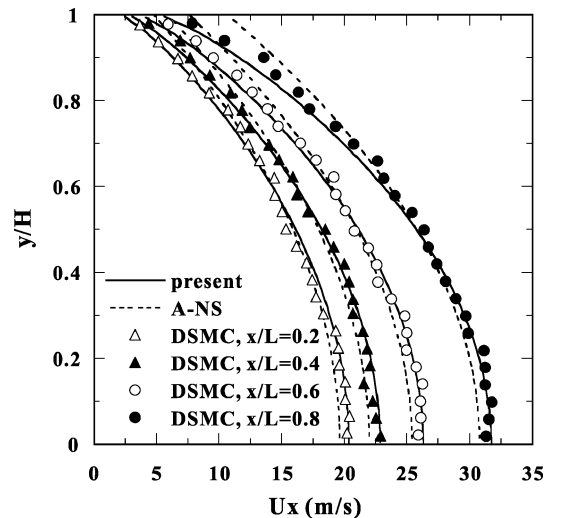


Fig. 1 Comparison of x -velocity distributions for a short microchannel flow.

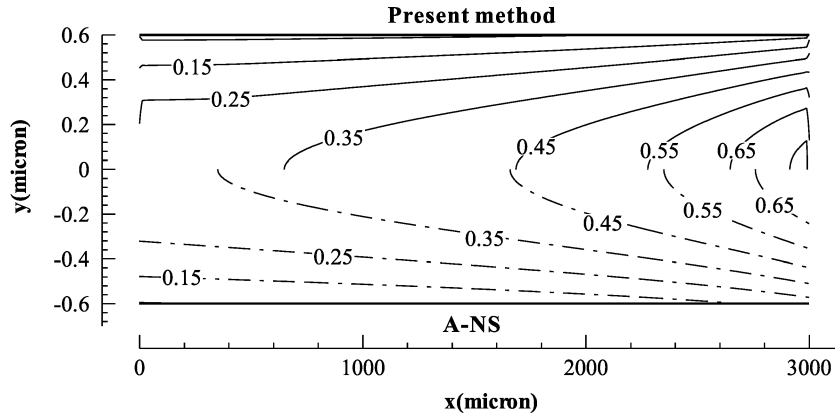
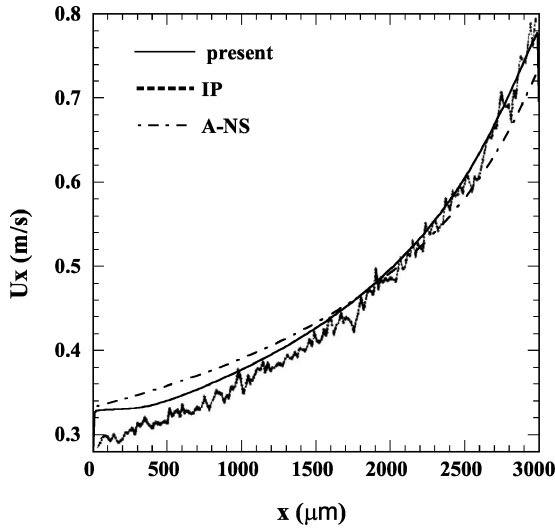
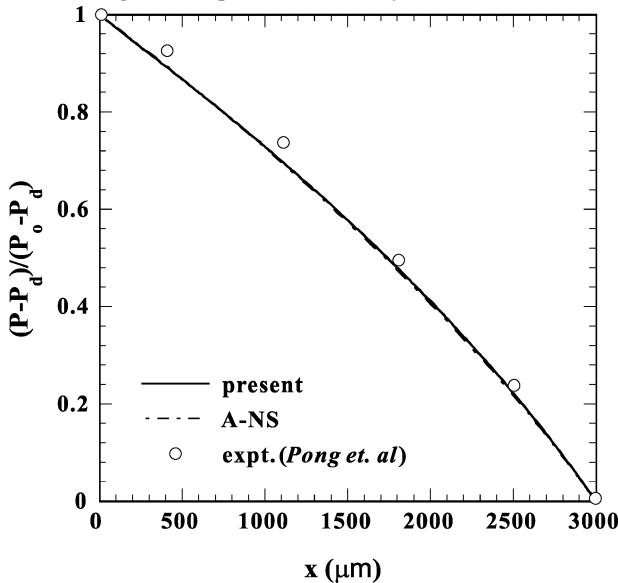
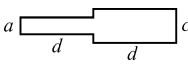
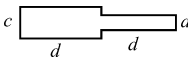
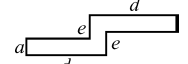
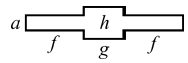
Fig. 2 Contours of x velocity for a long microchannel flow.Fig. 3 Comparison of x -velocity distributions.

Fig. 4 Comparison of pressure distributions.

300 K is chosen to be $\mu = 22.12 \times 10^{-6}$ kg/m·s to fit the parameters used in Ref. 7. The Knudsen number at the mean pressure $P = (P_0 + P_d)/2$ is $Kn = 0.03$. For the IP calculation,⁷ a rectangular grid system of 250×20 cells was employed. For the present method, a rectangular grid system of 251×21 grids is employed. CPU time required for the present method was about 53 h.

Figure 2 shows x -velocity contours from the present method and those from the analytical solution of the Navier–Stokes equations

Table 1 Geometry of microfluidic systems

Case	Shape	Dimension, μm
2		$a = 0.5$ $c = 1.0$ $d = 7.5$
3		$a = 0.5$ $c = 1.0$ $d = 7.5$
4		$a = 0.5$ $d = 7.5$ $e = 1.0$
5		$a = 0.5$ $f = 6.25$ $g = 2.5$ $h = 1.5$

with slip boundary conditions (see Ref. 16). Figure 3 shows centerline x -velocity distributions from three different methods. The solid line is the result of the present method and the dot-dashed line is that from the analytical solution of the Navier–Stokes equations with slip boundary conditions. The dotted line is the result from the IP method.⁷ The results from three different methods show relatively good agreement. Figure 4 shows centerline pressure distributions from the two different methods together with experiments.²⁵ Note that the results from the two numerical methods are almost identical and successfully capture the nonlinearity in the pressure distribution observed in the experiment. Although not shown here, the pressure distribution from the IP method⁷ is also almost identical, except that it has some statistical scatterings.

To investigate low-speed gas flows in microfluidic systems consisting of microchannels in series, four cases shown in Table 1 are considered. The gas is air with the viscosity index of $\omega = 0.77$. The pressures at the inlet and exit are 2.5×10^5 and 1.0×10^5 Pa, respectively. The temperature at the inlet and at the surface is 300 K. The average Knudsen number calculated using the flow variables at the mean pressure $P = (P_0 + P_d)/2$ is $Kn = 0.06$.

Case 2 is a sudden expansion consisting of two equal-length microchannels with a height ratio of two in series. For the calculations, only the upper-half portion of the flow domain is considered, with a symmetric boundary condition along the centerline. For the DSMC calculation, a rectangular grid system of $165 \times 25 + 165 \times 50$ cells is employed with about 350,000 particles and 36,000 sampling time steps (average sampling size of 1.0×10^6 per cell) after 40,000 time steps of development. For the present method, a rectangular grid system of $165 \times 26 + 165 \times 51$ grids is employed. Figure 5 shows x -velocity contours from the present and the DSMC methods. CPU times required for the DSMC and the present methods were about 31.1 and 11.5 h, respectively. The contours in the upper-half portion of Fig. 5 are results of the present method, and those in the lower-half portion are results calculated by the DSMC method. Figure 6 compares x -velocity distributions along the centerline of the channel

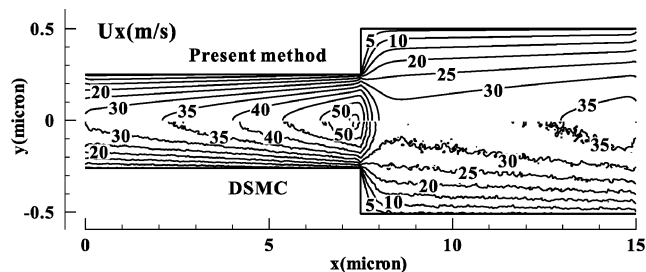
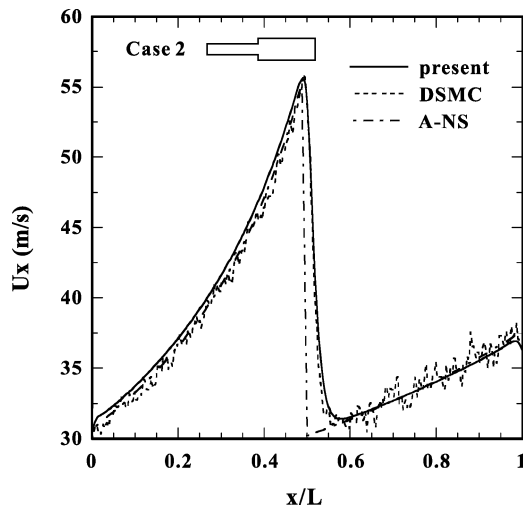
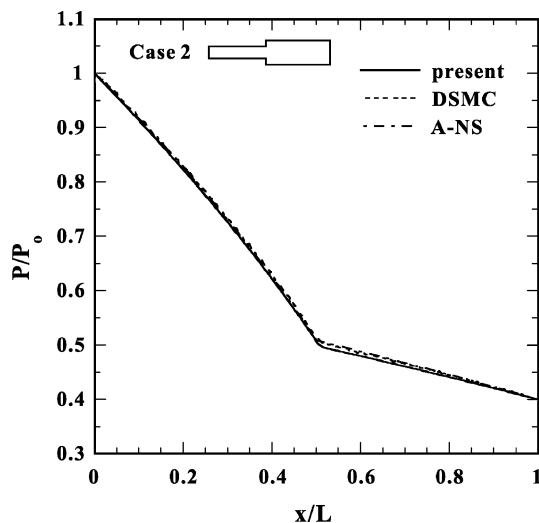
Fig. 5 Comparison of x -velocity contours for case 2.Fig. 6 Comparison of x -velocity distributions for case 2.

Fig. 7 Comparison of pressure distributions for case 2.

from three different methods. The results for the analytical solution of the Navier–Stokes equations with slip boundary conditions are obtained by assuming that both of the pressures at the junction and the mass fluxes through the two channels are equal, which means entrance and exit effects are neglected. Figure 7 compares pressure distributions in the channel from three different methods. As expected, the most of the pressure drop occurs in the first channel. The flow accelerates through the channel, and the velocity drops sharply at the junction where the flow expands. Note that the results from the present and the DSMC methods compare very well. The velocity distribution from the analytical solution of the Navier–Stokes equations shows relatively good agreement, except at the junction, due to entrance and exit effects. Note that the analytical solution of the Navier–Stokes equations with slip boundary conditions, which is suitable for fully developed flows, can give good results in predicting the geometrically complex flows.

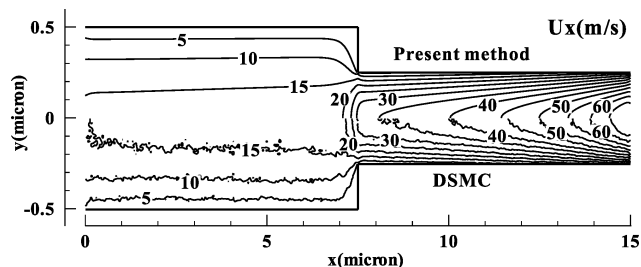
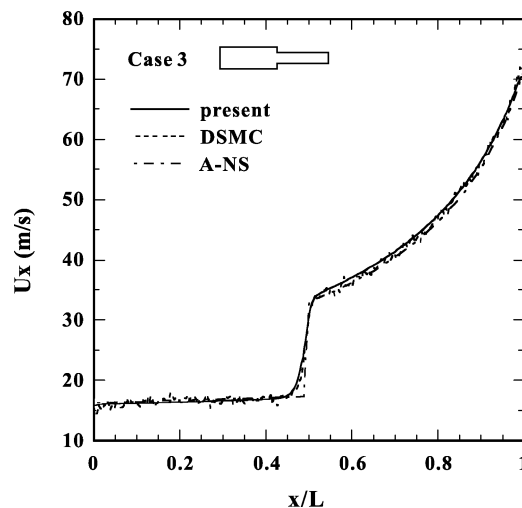
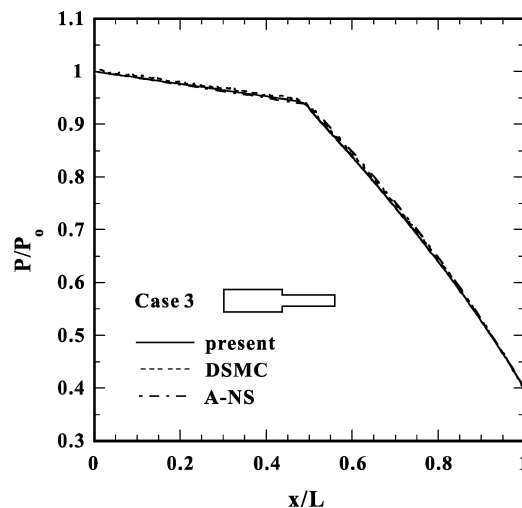
Fig. 8 Comparison of x -velocity contours for case 3.Fig. 9 Comparison of x -velocity distributions for case 3.

Fig. 10 Comparison of pressure distributions for case 3.

Case 3 is a sudden contraction consisting of two equal-length microchannels with a height ratio of 0.5 in series. For the calculations, only the upper-half portion of the flow domain is considered, with a symmetric boundary condition along the centerline. For the DSMC calculation, a rectangular grid system of $165 \times 50 + 165 \times 25$ cells is employed with about 330,000 particles and 38,000 sampling time steps (average sampling size of 1.0×10^6 per cell) after 40,000 time steps of development. For the present method, a rectangular grid system of $165 \times 51 + 165 \times 26$ grids is employed. CPU times required for the DSMC and the present methods were about 39.4 and 14.24 h, respectively. Figure 8 shows x -velocity contours from the present and the DSMC methods. The contours in the upper-half portion of Fig. 8 are results of the present method, and those in the lower-half portion are results calculated by the DSMC method. Figure 9 shows a comparison of x -velocity distributions along the centerline of the channel from three different distributions. Figure 10

shows a comparison of pressure distributions in the channel from three different methods. In this case, most of the pressure drop occurs in the second channel. The lateral change in the x velocity is very small in the first channel, and the flow accelerates in the second channel. Again, note that the results from the present and the DSMC methods compare very well.

Case 4 is a microfluidic system consisted of two 90-deg bends in series. Although the total width of the system is $14\ \mu\text{m}$, the distance from the entrance to the exit along the centerline of the channel is $15\ \mu\text{m}$. A rectangular grid system of $201 \times 41 + 41 \times 121 + 201 \times 41$ grids is employed for the calculation. CPU time required was about 11.2 h. Figure 11 shows pressure contours in the channel. The pressure is normalized by the inlet pressure. The contour line of $P/P_0 = 0.7$ is located at the entrance of the last channel, which indicates a nonlinear pressure distribution along the

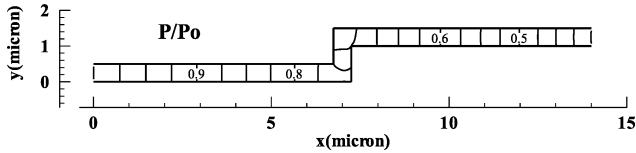


Fig. 11 Pressure contours for case 4.

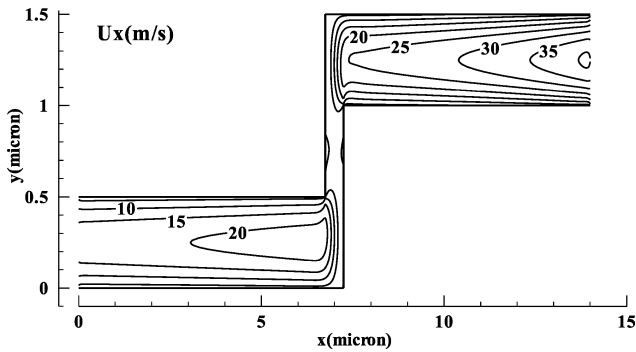


Fig. 12 Distributions of x velocity for case 4.

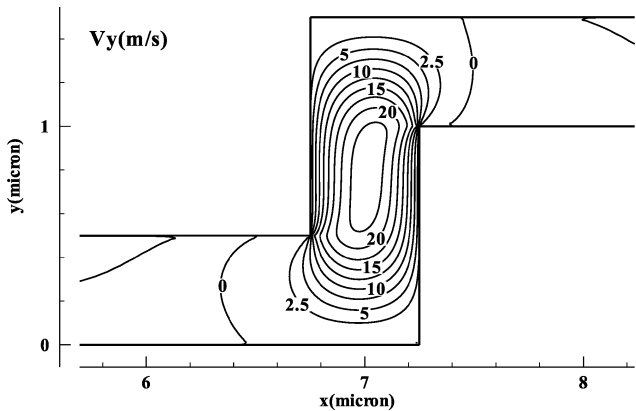


Fig. 13 Distributions of y velocity for case 4.

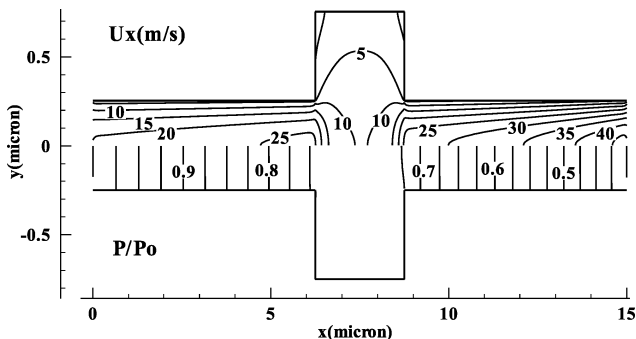


Fig. 14 Contours of x velocity and pressure for case 5.

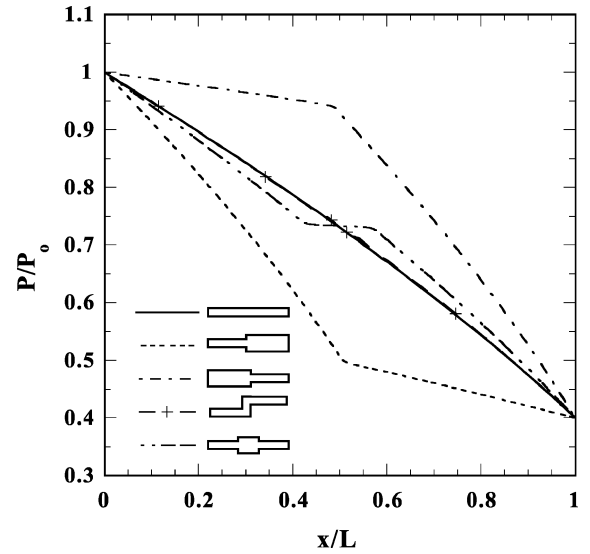


Fig. 15 Comparison of pressure distributions for various microfluidic systems.

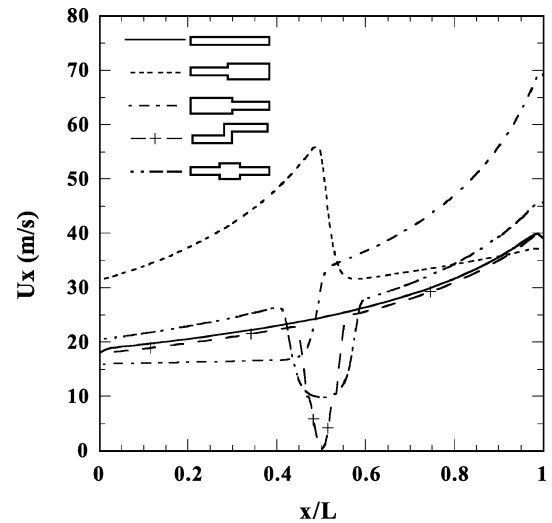


Fig. 16 Comparison of x -velocity distributions for various microfluidic systems.

centerline. Figure 12 shows x -velocity contours, and Fig. 13 shows y -velocity contours around the bends.

For case 5, a rectangular grid system of $161 \times 21 + 161 \times 61 + 161 \times 21$ grids is employed, and only the upper-half portion of the flow domain is considered with a symmetric boundary condition along the centerline. CPU time required was about 36.5 h. Figure 14 shows x -velocity and pressure contours for case 5. The upper-half portion shows the x -velocity contours and the lower-half shows the pressure contours. The height of the short channel at the center is three times that of the other two channels. Note that the variation of the pressure in the center channel is very small, and the channel acts like a reservoir. Again, the $P/P_0 = 0.7$ contour line is located near the entrance of the last channel and indicates the nonlinear pressure distribution in the channel.

Figure 15 shows a comparison of the pressure distribution along the centerline of various microfluidic systems. Figure 16 shows a comparison of x -velocity distributions along the centerline of various microfluidic systems. In the case of the microfluidic system consisting of two 90-deg bends in series (case 4), x is the distance measured from the entrance along the centerline. Note that the pressure distribution for the microfluidic system consisting of two 90-deg bends in series is almost identical to that of the simple channel with the same centerline distance from the entrance to the exit. For these two cases, the centerline x -velocity distributions are also very

similar, except for the region around the bends where the direction of the flow is changed. The pressure distribution for case 4 shows that the variation of the pressure in the center channel is very small, although there is a large change in the x -velocity distribution as shown in Fig. 16. The sudden contraction case shows the highest exit velocity, whereas the sudden expansion shows the lowest exit velocity.

V. Conclusions

A finite difference method coupled with the discrete-ordinate method is employed to analyze low-speed gas flows in various microfluidic systems consisting of microchannels in series. Calculations are made for simple microchannel flows with small and large length-to-height ratios. The results compare well with those from the DSMC method, an analytical solution of the Navier–Stokes equations with slip boundary conditions, and available experimental data. The present method is then applied to various microfluidic systems consisting of microchannels in series such as a sudden expansion, a sudden contraction, and a system with two 90-deg bends. The advantage of the present method is that it does not suffer from statistical noise, which is common in particle-based methods. The CPU times required for the present method were about one-third of those for the DSMC method. The present method can be used to analyze low-speed flows in which the velocity of the flowfield is less than 1 m/s. It would be almost impossible to analyze such flowfields using the DSMC method. It is also shown that the analytical solution of the Navier–Stokes equations with slip boundary conditions, which is suited for fully developed flows, can give good results in predicting the geometrically complex flows such as a sudden expansion and a sudden contraction.

Acknowledgments

This work was sponsored by Grant R05-2003-000-10145-0 from the Basic Research Program of the Korea Science and Engineering Foundation.

References

- ¹Bird, G. A., *Molecular Gas Dynamics and the Direct Simulation of Gas Flows*, Clarendon, Oxford, England, U.K., 1994.
- ²Ikegawa, M., and Kobayashi, J., "Development of a Rarefied Flow Simulator Using the Direct-Simulation Monte-Carlo Method," *JSME International Journal*, Series 2, Vol. 33, No. 3, 1990, pp. 463, 467.
- ³Piekos, E. S., and Breuer, K. S., "Numerical Modeling of Micromechanical Devices Using the Direct Simulation Monte Carlo Method," *Transactions of the ASME*, Vol. 118, Sept. 1996, pp. 464, 469.
- ⁴Oh, C. K., Oran, E. S., and Sinkovits, R. S., "Computations of High-Speed, High Knudsen Number Microchannel Flows," *Journal of Thermophysics and Heat Transfer*, Vol. 11, No. 4, 1997, pp. 497, 505.
- ⁵Nance, P. R., Hash, D. B., and Hassan, H. A., "Role of Boundary Conditions in Monte Carlo Simulation of Microelectromechanical Systems," *Journal of Thermophysics and Heat Transfer*, Vol. 12, No. 3, 1998, pp. 447, 449.
- ⁶Fan, J., and Shen, C., "Statistical Simulation of Low-Speed Unidirectional Flows in Transition Regime," *Rarefied Gas Dynamics*, edited by R. Brun, R. Campargue, R. Gatignol, and J. C. Lengrand, Vol. 2, Cepadues-Editions, Toulouse, France, 1999, pp. 245, 252.
- ⁷Cai, C., Boyd, I. D., Fan, J., and Candler, G. V., "Direct Simulation Methods for Low-Speed Microchannel Flows," *Journal of Thermophysics and Heat Transfer*, Vol. 14, No. 3, 2000, pp. 368, 378.
- ⁸Sun, Q., Boyd, I. D., and Candler, G. V., "Numerical Simulation of Gas Flow Over Microscale Airfoils," *Journal of Thermophysics and Heat Transfer*, Vol. 16, No. 2, 1992, pp. 171–179.
- ⁹Sun, Q., and Boyd, I. D., "Drag on a Flat Plate in Low-Reynolds-Number Gas Flows," *AIAA Journal*, Vol. 42, No. 6, 1994, pp. 1066–1072.
- ¹⁰Sun, Q., and Boyd, I. D., "Flat-Plate Aerodynamics at Very Low Reynolds Number," *Journal of Fluid Mechanics*, Vol. 502, 1994, pp. 199–206.
- ¹¹Chung, C. H., De Witt, K. J., Jeng, D. R., and Keith, T. G., Jr., "Numerical Analysis of Rarefied Gas Flow Through Two-Dimensional Nozzles," *Journal of Propulsion and Power*, Vol. 11, No. 1, 1995, pp. 71, 78.
- ¹²Huang, A. B., "The Discrete Ordinate Method for the Linearized Boundary Value Problems in Kinetic Theory of Gases," *Rarefied Gas Dynamics and Plasma Lab., School of Aerospace Engineering, Georgia Inst. of Technology, Rept. 4*, Atlanta, GA, 1967.
- ¹³Bhatnagar, P. L., Gross, E. P., and Krook, M., "A Model for Collision Processes in Gases. I. Small Amplitude Processes in Charged and Neutral One-Component Systems," *Physical Review*, Vol. 94, No. 3, 1954, pp. 511, 525.
- ¹⁴Huang, A. B., and Giddens, D. P., "A New Table for a Modified (Half-Range) Gauss–Hermite Quadrature with an Evaluation of the Integral," *Journal of Mathematics and Physics*, Vol. 47, March 1968, pp. 213, 218.
- ¹⁵Shizgal, B., "A Gaussian Quadrature Procedure for Use in the Solution of the Boltzmann Equation and Related Problems," *Journal of Computational Physics*, Vol. 41, No. 2, 1981, pp. 309, 328.
- ¹⁶Arkilic, E. B., Schmidt, M. A., and Breuer, K. S., "Gaseous Slip Flow in Long Microchannels," *Journal of Microelectromechanical Systems*, Vol. 6, No. 2, 1977, pp. 167, 178.
- ¹⁷Chu, C. K., "Kinetic-Theoretic Description of the Formation of a Shock Wave," *Physics of Fluids*, Vol. 8, No. 1, 1965, pp. 12, 22.
- ¹⁸Chung, C. H., "Numerical Simulation of Rarefied Gas Flow Through Nozzles and Over Submerged Bodies," Ph.D. Dissertation, Dept. of Chemical Engineering, Univ. of Toledo, Toledo, OH, June 1990.
- ¹⁹Chapman, S., and Cowling, T. G., *The Mathematical Theory of Non-Uniform Gases*, Cambridge Univ. Press, London, 1958, pp. 218, 234.
- ²⁰Bird, G. A., "Monte Carlo Simulation in an Engineering Context," *Rarefied Gas Dynamics*, edited by S. S. Fisher, Vol. 74, Pt. I, Progress in Astronautics and Aeronautics AIAA, New York, 1981, pp. 239, 255.
- ²¹Bird, G. A., "Perception of Numerical Methods in Rarefied Gas Dynamics," *Rarefied Gas Dynamics*, edited by E. P. Muntz, D. P. Weaver, and D. H. Campbell, Vol. 118, Progress in Astronautics and Aeronautics, AIAA, Washington, DC, 1989, pp. 211, 226.
- ²²Chung, C. H., De Witt, K. J., Stubbs, R. M., and Penko, P. F., "Simulation of Overexpanded Low-Density Nozzle Plume Flow," *AIAA Journal*, Vol. 33, No. 9, 1995, pp. 1646, 1650.
- ²³Chung, C. H., Kim, S. C., De Witt, K. J., and Nagamatsu, H. T., "Numerical Analysis of Hypersonic Low-Density Scramjet Inlet Flow," *Journal of Spacecraft and Rockets*, Vol. 32, No. 1, 1995, pp. 60, 66.
- ²⁴Atassi, H., and Shen, S. F., "A Unified Kinetic Theory Approach to External Rarefied Gas Flows. Part 1. Derivation of Hydrodynamic Equations," *Journal of Fluid Mechanics*, Vol. 53, Pt. 3, 1972, pp. 417, 431.
- ²⁵Pong, K. C., Ho, C. M., Liu, J. Q., and Tai, Y. C., "Nonlinear Pressure Distribution in Uniform Microchannels," *Application of Microfabrication to Fluid Mechanics*, Division (FED), Vol. 197, American Society of Mechanical Engineers, New York, 1994, pp. 51, 56.